Proceedings of ITC18,2008

Micro-spectroscopic Investigation of the Plasma-surface Interaction in the Microwave Carbothermic Reduction of the Powdered Magnetite

Akihiro Matsubara[1], Kazuya Nakayama[1], Shigeki Okajima[1], Sadatsugu Takayama[2], and Motoyasu Sato[2]

[1]*Chubu University, 1200, Matsumoto, Kasugai, Aichi, 487-8501, Japan*

[2]*National Institute for Fusion Science, 322-6 Oroshi, Toki, Gifu, 509-5292, Japan*

The plasma-surface interaction in microwave carbothermic reduction of magnetite was experimentally investigated with the Integrated Microscopic Imaging System. It was found that luminous body with burst/jet structure is formed on the specimen during reduction period. Its emission spectrum has a continuous spectrum of thermal radiation, and laser beams are scattered significantly by the luminous body. These facts suggest presence of plasma-powder mixture. The formation of the mixture, position in dust plasma, and the relation to the PSI in fusion science are described.

Keywords: plasma-surface interaction, plasma-powder particle mixture, microwave carbothermic reduction, spectroscopic measurement, luminous body, dust plasma, self-organization.

1. Introduction

Plasma-surface interaction is one of crucial issues in fusion research as well as plasma processing, but in some cases it has been also studied in the field of the material processing associated with thermally activated processes based on microwave heating. A typical example is microwave iron production presented here. High-purity pig irons have been produced successfully in a multimode microwave test reactor from powdered iron ores (magnetite) with carbon as a reducing agent in a nitrogen atmospheric pressure [1]. The microwave iron making has the advantage that the CO_2 emissions can be reduced by tens of percent compared with that in conventional blast furnaces, if the electric power for the microwave is generated by renewable energy, such as solar, hydro and nuclear power. A feature of the microwave method is the sudden rise in temperature of the material surface from ~700 °C to ~1000 °C accompanied by light emission of atmospheric plasma [2]. The nature of the temperature jump has been seen simply an emergence of an additional energy flow to the material through the plasma. Such plasma has been observed in almost all similar experiments.

In order to investigate the plasma-surface interaction in the microwave iron making, visible emission spectroscopy has been introduced. The light emission after the temperature jump consists of strong atomic/molecular lines. These lines have been well assigned as spectra listed in the spectrum database based on the spark and arc discharge [2], indicating the presence of plasma electrons with several electron volts in the electron temperature. The multipoint pyrometric and spectroscopic measurements demonstrated that the microwave heating mode changes from direct volumetric heating by microwave into surface heating by plasma, when the atmospheric plasma is generated [2]. It was found that the structure of emission spectrum near-UV range (240 nm - 310 nm) changes drastically from the continuous spectrum to line spectra of iron, with progressing reduction process [2].

The present paper provides micro-spectroscopic observation indicating that the plasma formed on the material takes on an aspect of plasma-powder mixture. It will be shown that burst/jet structure with continuous emission spectrum appears just above the specimen during reduction dominated period. The aspect of plasma-powder mixture dismisses the simple view that the plasma is just an independent medium as a microwave absorber for heating the material; rather, that aspect requires consideration of modification of microwave propagation and absorption in the plasma-powder mixture. Such feedback leads to the self-organization of the three-body mixture consisting of the microwave field, plasma-powder mixture, and powdered-material (specimen). It will also described about the position in the category so called *dust plasma*. The relation to the plasma-surface interaction in fusion devices also briefly mentioned.

2. Experimental setup

Figure 1 shows the microwave single mode cavity (TE_{103} at cw 2.45 GHz) and its diagnostics system located at the National Institute for Fusion Science. In this experiment the specimen was set at the anti-node of the electric-field standing wave, i.e., the electric field heating.

author's e-mail: MATSUBARA.Akihiro@sti.chubu.ac.jp

The specimen was made of magnetite (Fe_3O_4) and graphite powders of which grain sizes were <1 μm and *ca.* 5 μm, respectively. The mixing ratio was M_{Fe3O4} : M_C = 90 : 10 by mass. Corresponding mol ratio was n_{Fe3O4} : n_C = 1.0 : 2.0 that is equivalent mole portions for the carbothermic reduction of magnetite, $Fe_3O_4 + 2C \rightarrow 3Fe + 2CO_2$ − 317 kJ/mol. The composite powder (total mass: 0.619 g) was shaped into a cylindrical rod of 8-mm in diameter and 10-mm in length. The specimen was set inside the quartz cell (12.5 mm in inner diameter and 200 mm in length). Before starting the microwave irradiation, the quartz cell was evacuated by the rotary pump and refilled with helium gas. During the irradiation, a continuous helium gas flow of 20 ml/min was used with a pressure a little higher than ambient pressure.

The microscopic spectroscopy was performed with the Integrated Microscopic Imaging System as shown in Fig. 2. A feature of it is integration of a microscope and a 2D-imaging spectrometer. This allows us to observe emission spectrum in parallel with watching the appearance of the specimen through the microscope image. The emission light from the specimen is condensed by the objective lens; then, it is split in two by half mirror. The transmitted light is detected by the microscope, and the reflected light is introduced into the magnification lens, scanning mirror, and finally the imaging spectrometer that is a lens-slit Czerny-Turner configuration. The camera lens as the collimator in the spectrometer minimizes aberration of astigmatism due to the collimator mirror in a common spectrometer. In present experiment no mirror scanning mode is taken for enhancing dynamic range. The slit-shaped observation region on the specimen is fixed at a center of the observation region of the microscope [see Fig. 4]. The exposure time was 20 ms for the microscope, and 580 ms for the spectrometer.

Two InGaAs pyrometers [labeled as IR1 and IR2 shown in Fig. 1] were taken for measurement of the specimen temperature. IR1 and IR2 were directed to the specimen top surface and side surface, respectively. The neutral gas pressure in the cell was monitored with the electrical-resistance strain-gage type transducer. Flow rate of exhaust gas was measured by the mass flow meter, and exhaust gas analysis was performed with the quadrupole mass analyzer.

3. Experimental results

Figure 3 shows time evolutions of various parameters measured during the heating. There are three stages associated with the change of phenomena as I - III depicted schematically above the upper axis of Fig. 3(a):

I. Pre-reduction stage (t < 200 s) characterized by microwave direct volumetric heating.

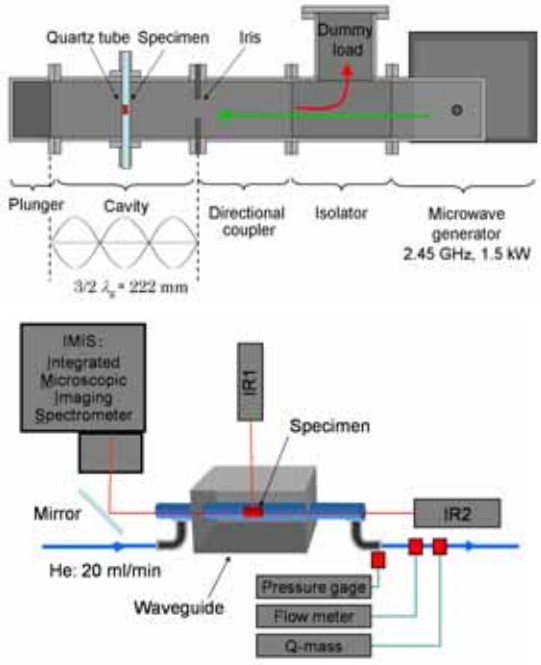

Fig. 1. Experimental setup of the microwave heating in the single mode cavity in the upper frame and diagnostics system in the lower frame.

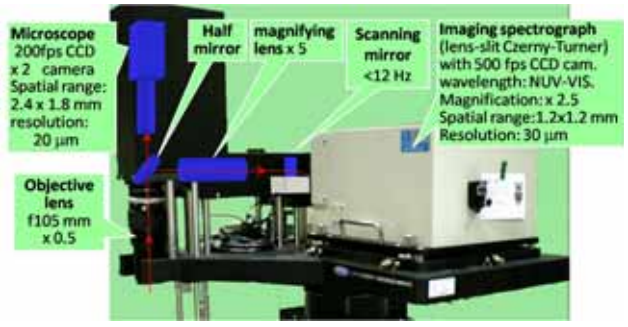

Fig. 2. Integrated Microscopic Imaging Spectrometer and its structure and specification.

II. Reduction-dominated stage (t = 200 ~ 320 s) with the significant plasma surface interaction and exhaust gas generation.

III. Post-reduction dominated stage (t > 320 s).

These stages are equivalent fundamentally to that found in previous experiments for microwave iron making [2].

In the first stage, the temperature of the top and side surfaces increases in the same way as shown in Fig. 3(a), indicating homogeneous direct microwave heating. There are almost no exhausted gases detected.

The beginning of the stage II is triggered by the plasma ignition. As shown in Fig. 3(a) the temperature of the top surface inherently jumps up from 512 °C at t = 200 s, and it reaches 1160 °C within 4 s. The side-surface temperature rises gradually and reaches 1160 °C taking for ~100 s. The exhaust gas flow rate keeps higher level

in this stage as shown Fig. 3(b). In addition constituent of the exhaust gas is mainly CO_2 and CO [see Figs. 3(c)-3(f)]. It should be noted that the exhaust flow rate is several times overestimated because of the mass flow meter is for helium gas. The time when CO_2- and CO- gas arrives at the flow meter is supposed at ~222 s, corresponding to the sudden rise of the flow rate. By using the flow rate of ~50 ml/min before the sudden rise, the total amount of gas generated in this period (~2 min) can be comparable within the order of magnitude to the amount of mass loss of the specimen (0.16 g); thus it is appropriate interpretation that the reduction process is dominated in this period.

Figure 4(a) shows the typical microscope image captured by IMIS during the stage II. The field of view was placed to include the top surface of the cylindrical specimen. It is found that the burst occurs frequently with jet structure. The duration of the burst is less than 50 ms in this case, but in some cases it reaches 100 ms. It is also found that the space just above the specimen is filled by luminous body. The spectral image displayed in Fig. 4(c) for which the field of view is depicted as the vertical line in Fig. 4(a) indicates that there is strong continuous spectrum corresponding to that luminous body. In addition a few line emission spectra are superimposed on the continuous spectrum. Figure 4(b) shows the spectrum above the specimen [y = 1.33 mm; indicated by the marker in Fig. 4(c)]. Peaks with arrow can be assigned as iron atomic spectrum. The strong peaks at 569 nm and 590 nm are Na I. Although the constituent concentration of sodium is under 0.01% in the raw material, transition probability for Na I (3s-3p) is quite large; it makes the intensity of the spectrum stronger.

As the stage changes into III (post reduction period), the exhaust gas flow rate decreases, and finally almost no exhaust gas is generated [see Fig. 3(b)]. It should be noted that the bright plasma emission around the specimen was still visible with the naked eye; however as shown in Fig. 5(a) in microscopic observation it is found that there is no luminous body as found in the reduction period of stage II. In fact the spectral image has no strong continuous spectrum as seen in stage II, rather molecular band spectra of both C_2 ($A^3\Pi_g$ - $X\,^3\Pi_u$) and CO ($B^1\Sigma$-$A^1\Pi$) appear clearly at the edge of the material.

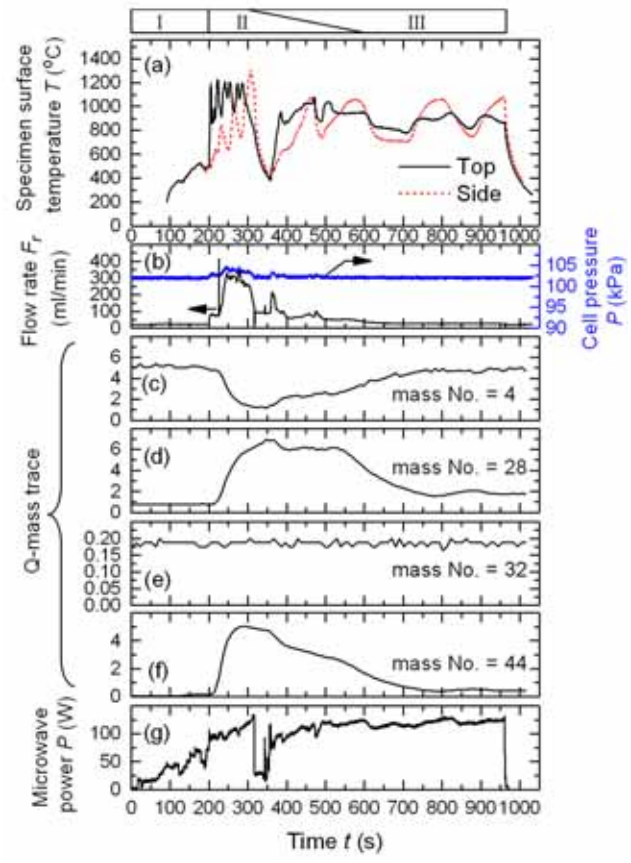

Fig. 3. Evolution of specimen temperatures in (a), the exhaust flow rate and cell pressure in (b), relative intensities of the signal in the quadrupole mass-analyzer in (c) – (f), and the net microwave power absorbed in the single mode cavity in (g).

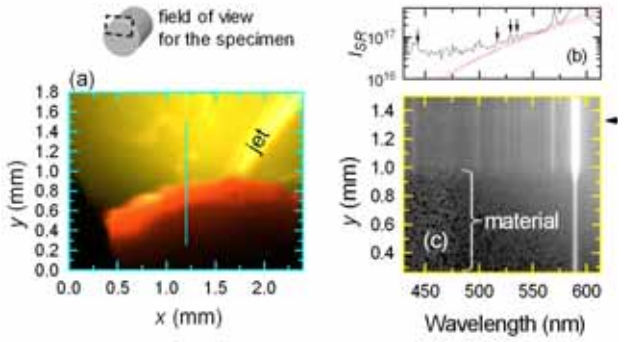

Fig. 4. Typical visible (a) and spectral (c) images of the upper part of specimen for the reduction dominated period (the stage II; t = 234 s). The vertical line in (a) depicts the field of view for the spectral image of (c). Arrows in (b) shows spectra assigned as Fe I. The unit of I_{SR} is photons m^{-2} s^{-1} nm^{-1} sr^{-1}.

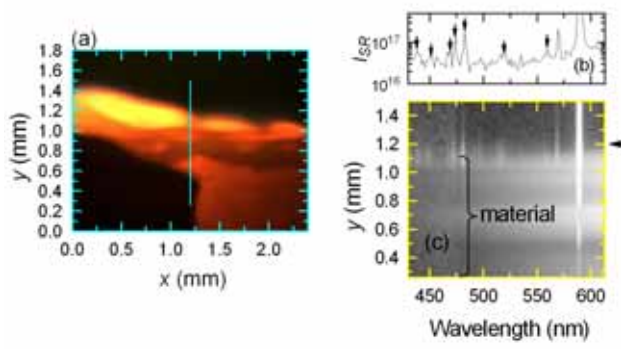

Fig. 5. Typical visible (a) and spectral (c) images captured in the post reduction period (the stage III; t = 505 s). Arrows in (b) shows spectra assigned as CO ($B^1\Sigma$-$A^1\Pi$) and C_2 ($A^3\Pi_g$ - $X\,^3\Pi_u$).

4. Discussion

The luminous body (with burst and jet) and continuous spectrum just above the specimen during reduction period (the stage II) imply presence of plasma-powder mixture generated by strong plasma-surface interaction. A part of the continuous spectrum can be due to the thermal radiation of the powder in the plasma. Three thermal radiation spectrums for temperature range of 1200 - 1400 °C and emissivity range of 0.1 - 1.0 are drawn as red dotted lines in Fig. 4(b). That temperature range is comparable to or somewhat higher than that of specimen temperature measured by pyrometers. This situation inspires us to consider inclusion of powder particles from the specimen into the plasma.

The intensity of the observed spectrum is higher than that of the thermal spectrum for shorter wavelength. This can be connected with the results reported in the previous paper [2]. It was found that the intensity of continuous emission spectrum near-UV range (240 nm - 310 nm) is more three order magnitude larger than that of black body spectrum. A candidate of the continuous spectrum was considered as a cathodoluminescence of magnetite (reported wavelength range: 310-620 nm with twin peaks at 390 nm and 480 nm) due to the impingement of a plasma electron onto the specimen surface of magnetite.

The view of the plasma-powder mixture has been supported by the similar experiment for the measurement of CO_2 concentration with CO_2-laser absorption. An He-Ne laser beam (633 nm) was aligned along the CO_2 laser beam, in order to monitor influence of laser-light scattering due to the powder particles inside the plasma. It was found that the transmissivities for both CO_2- and He-Ne lasers drop to 0.1 during reduction dominated period. This value is much less than that based on gas absorption, indicating almost scattering (~ 90 %) by powder particle.

The plasma-powder mixture can be formed in such a way that the powder is blown into the space by the burst and jet as mentioned above. The burst and jet can result from reduction reaction and/or an adiabatic expansion by localized heating (likely due to a micro scale arc discharge), and those consist of CO/CO_2 gas and powder particles. On the other hand disappearance luminous body in the post reduction period (stage III) will be explained as depletion of the raw powder (i.e., as progress of reduction). Emergence of molecular spectrum of CO ($B^1\Sigma$-$A^1\Pi$) indicates that electron plasma temperature is higher for post reduction period than that for the reduction period. The waning of the plasma-powder interaction suppresses the power loss through thermal radiation and reduction reaction of the powder particle in the plasma.

It would be mentioned about the possibility that the plasma-powder mixture plays not merely a part of microwave absorber/heater; rather, it behaves as a component in self-organization of the system consisting of microwave field, plasma-powder mixture, and powder material (specimen). The hot spots on the surface causing the burst/jet can be attributed to microwave focusing due to a kind of edge effects; however the propagation and absorption of microwave itself will be modified by the plasma-powder mixture.

The plasma-powder mixture presented here would be categorized into *hot dust plasma*, since thermal- and secondary-electron emissions should not be neglected [3]. There are some similarities with a hot-dust plasma so called *ball lightning* generated in the concentrated microwave field [4, 5]. The luminescence of the ball lightning has been explained as chemical emission due to re-oxidation of nano-particles generated by reduction reaction through the localized arcing in the surface layer of material. The micro-scale structure observed in present experiment supports qualitatively above explanation.

Finally, relationship to the plasma-surface interaction in fusion science would be mentioned briefly. The condition that plasma faces to the metal oxide-graphite mixture can be materialized in fusion device, if graphite particles are re-deposited on or implanted into metal oxide layer on the first wall. Formation of such metal-oxide layer is supposed to be rare case depending on leak of air or H_2O. When the significant heat flux from the plasma typically induced by an edge localized mode (ELM) strikes the deposition area, the metal oxide is reduced by graphite and resultant CO/CO_2 gas takes the deposited particles toward the plasma. The contamination of the dust particles can change the propagation and absorption of high frequency electromagnetic wave [6].

Acknowledgement

This research is supported in part by a Grant-in-Aid for Scientific Research on Priority Areas (465) of the Ministry of Education, Culture, Sports, Science and Technology in Japan.

References

[1] K. Nagata, *et al*., *Proc. of 4th Int. Cong. on Sci.&Tech. of Steel Making*, Gifu, 632 (2008).
[2] A. Matsubara1, *et al*., Plasma Fusion Res. **3**, S1085 (2008).
[3] P. K. Shukla, Phys Plasma **8**, 1791 (2001).
[4] J. Abrahamson and J. Dinniss, Nature **403** 519 (2000).
[5] V. Dikhtyar and E. Jerby, PRL **96** 045002 (2006).
[6] S. Takamura, J. Plasma Fusion Res. **78** 295 (2002).